Magnetization of negative magnetic arrays: Elliptical holes on a square lattice

I. Guedes,* N. J. Zaluzec, and M. Grimsditch
Materials Science Division, Argonne National Laboratory, Argonne, Illinois 60439-4845

V. Metlushko
Department of Electrical Engineering and Computer Science, University of Illinois at Chicago, Chicago, Illinois 60607 and Materials Science Division, Argonne National Laboratory, Argonne, Illinois 60439-4845

P. Vavassori
University of Ferrara, Ferrara, Italy

B. Ilic
School of Applied and Engineering Physics, Cornell University, Ithaca, New York 14853

P. Neuzil and R. Kumar
Institute of Microelectronics, 11 Science Park Road, Singapore 117685

(Received 12 May 2000)

The magnetic properties of an array of elliptical holes in an Fe film have been investigated using the diffracted magneto-optical Kerr effect (D-MOKE), Lorentz scanning transmission electron microscopy (LSTEM), and Brillouin scattering. In the absence of a comprehensive theory for magnetization or magnons in these materials, we find that our results can be fit by a semiquantitative analysis treating the system as uniform, anisotropic film. D-MOKE clearly shows that magnetization reversal occurs with extensive domain formation when the field is applied along the short axis of the elliptical holes, and almost no domain formation when it is along the long axis, while LSTEM demonstrates that the domain location is controlled by the elliptical holes. A theory of D-MOKE, which enables a quantitative analysis of loops, is also presented.

INTRODUCTION

The recent advances in lithographical techniques, which allow materials to be patterned at the nanometer length scale, have led to the fabrication of a number of novel systems. The magnetic properties of arrays of nanoparticles are receiving considerable attention due to their potential for practical applications. Arrays of holes have also been investigated but to a lesser extent.[1–7] From a fundamental standpoint the switching mechanisms during magnetization reversal is an important issue which is not yet well understood in these systems. It is now known that in dot arrays the shape of the individual elements plays a dominant role in the switching mechanism; equivalently it means that the shape anisotropy is an important contribution to the magnetic energy of the system. Here we investigate how the ''shape anisotropy'' affects the magnetic properties of an array of holes.

In Refs. 1–4 and 6,7 the domain structure that develops during switching in antidot arrays was investigated using magnetic force microscopy (MFM) and micromagnetic calculations. The magneto-optic Kerr effect (MOKE), or to be more precise D-MOKE (i.e., magneto-optic Kerr loops recorded on beams diffracted by the array), was used in Ref. 5 to investigate the magnetic properties of an array with circular holes. There it was found that the D-MOKE data provided information on the domains that form during switching: in that case, blade domains. In Ref. 5 a basic formalism for interpreting D-MOKE from positive dots was given; experimentally however, they found that the approach needed to be modified when dealing with a hole array. In that article the necessary changes were introduced in a qualitative manner.

Here we develop a firmer mathematical footing for relating D-MOKE loops with domain formation in a hole array. We also present a study of the magnetic properties of an Fe film in which elliptical holes, $\approx$200 nm wide by $\approx$800 nm long, have been fabricated on an almost square 1×1 μm lattice. Using MOKE and Brillouin scattering we have found that the patterned film develops an effective anisotropy of $\approx$200 G. The shape of the loops observed with D-MOKE provides a clear indication of domain formation, and the extension to the D-MOKE theory presented in Ref. 5 allows us to analyze the data in a semiquantitave manner and thereby infer the likely domain structure that develops during switching.

EXPERIMENTAL DETAILS

The fabrication techniques and D-MOKE system used for the experiments are identical to those described in Ref. 5. In this case the patterned Fe film was $\approx$60 nm thick with a 2.5 nm Cr overlayer having elliptical holes on a 1×1 μm lattice; the holes were $\approx$200 nm wide by $\approx$800 nm long. An SEM image of the sample is shown in Fig. 1.

Our Brillouin spectra were obtained on a $5+4$ pass tandem Fabry Perot interferometer (Ref. 8). The Brillouin technique measures excitations that are very closely related to the modes detected in ferromagnetic resonance (FMR) experi-

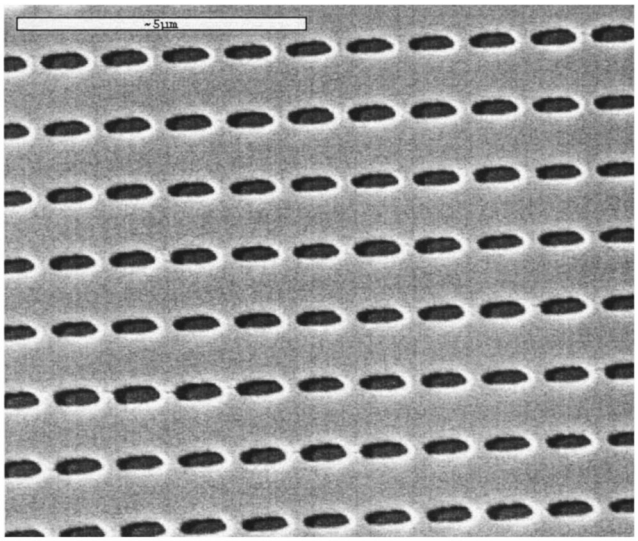

FIG. 1. SEM image of our array of elliptical holes in a 60 nm thick Fe film.

ments. Since the frequency of these modes depends on the magnetization and anisotropies, they can be used to probe the contributions to the magnetic energy. The theoretical consideration dealing with this issue will be presented together with the experimental results.

Specimens for Lorentz scanning transmission electron microscopy (LSTEM) were made by floating films off of the deposition substrate onto 3 mm diameter folding grids. The specimens were then studied in a field emission gun, VG HB 603 Z analytical electron microscope operating at 300 kV operating under UHV (~10–11 Torr) conditions. Magnetic domain images where obtained operating the microscope in a specialized zero field mode, which permits individual domains to be imaged in STEM using the Lorentz effect.[9]

RESULTS

Magnetization

In Figs. 2 and 3 we show the D-MOKE loops acquired with the applied field (H) along and perpendicular to the long axis of the ellipses, respectively. In each figure we show the loop obtained on the (a) unpatterned area of the sample, (b) the reflected beam from the patterned area (i.e., zeroth diffraction order), and (c) and (d) the first and second diffracted orders. In this section we will discuss only portions (a) and (b) of these figures. The higher order D-MOKE loops will be discussed later.

First we note that the unpatterned part of the film [loops 2(a) and 3(a)] has a small in-plane anisotropy with the hard axis along the direction parallel to the long axes of the ellipses. This small anisotropy is not uncommon in deposited thin films and is most likely produced by anisotropic strains or some degree of preferential orientation. We assume that the energy (E) of the film can be written

$$E = -M \cdot H + K \cos^2(\theta), \tag{1}$$

where M is the (uniform) magnetization of the film, H is the applied field, θ is the in-plane angle that the magnetization subtends with the direction of the long axis of the ellipses,

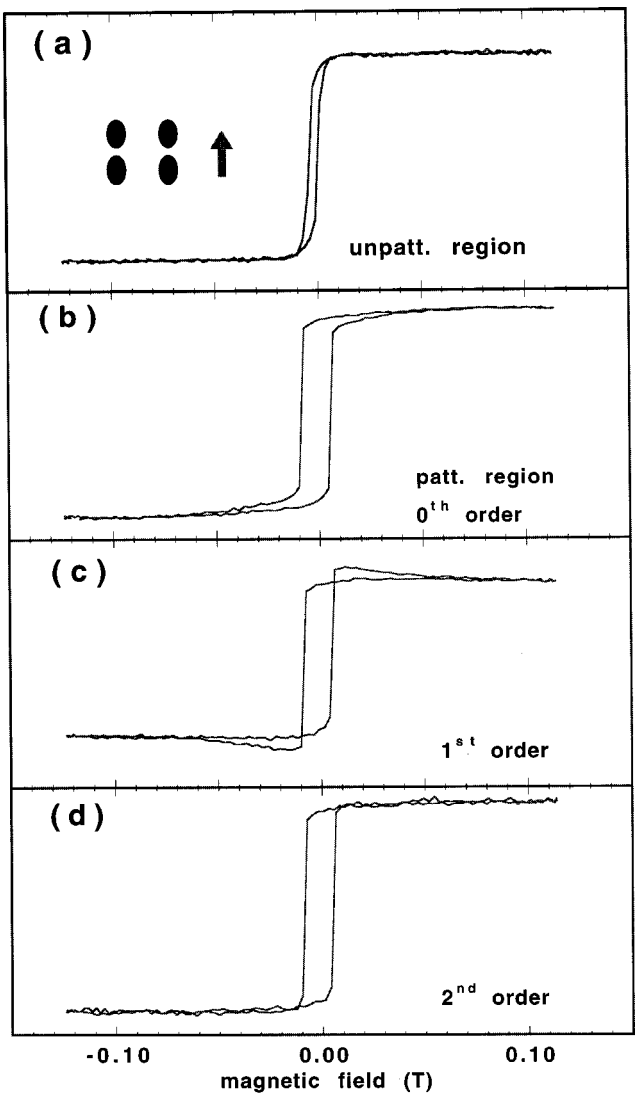

FIG. 2. MOKE loop on the unpatterned and D-MOKE loops of various orders from the patterned areas of the film. The applied field is along the long axis of the ellipses.

and K is the anisotropy constant. Equation (1) predicts that saturation occurs at $H = 2K/M$ when the field is applied along the hard axis. The magnitude of K/M, although it cannot be reliably extracted from Fig. 2(a), is positive but less than +50 G.

As will be shown below, the zeroth order D-MOKE loops [Figs. 2(b) and 3(b)] measure, as does conventional MOKE, the average magnetization. The two loops in Figs. 2(b) and 3(b) therefore show that the anisotropy in the patterned area is considerably larger and opposite in sign; i.e., the hard axis is now perpendicular to the long ellipse axis. Since saturation is reached at about 500 G in Fig. 3(b), we extract $K/M = -250$ G.

This hole-induced anisotropy can be understood as originating from the magnetostatic energy, associated with the surface ''magnetic charges'' that appear at the interface between a magnetized medium and vacuum (in the present case the hole edges). For our negative ellipse array there is considerably more ''magnetic surface charges'' when the system is magnetized perpendicular to the ellipses than when it is

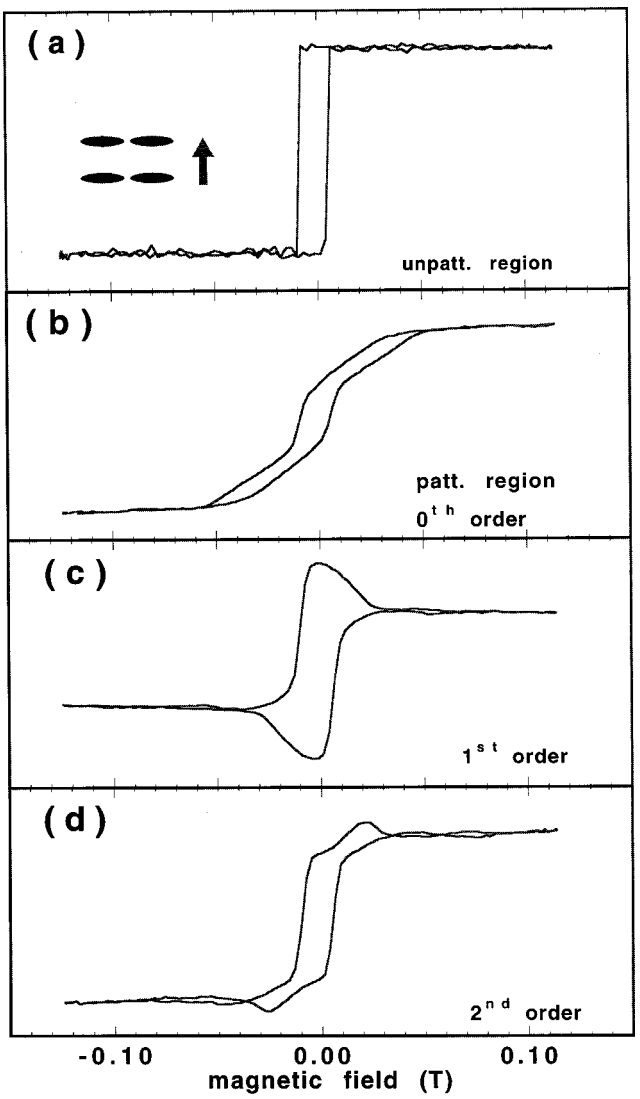

FIG. 3. MOKE loop on the unpatterned and D-MOKE loops of various orders from the patterned areas of the film. The applied field is along the short axis of the ellipses.

magnetized along the ellipse axis, so that the energy is lower for this latter case. The question that remains to be answered is if Eq. (1), which treats both the magnetization and the anisotropy as uniform throughout the film, is a suitable approximation to describe our, clearly nonuniform, hole array.

Magnetic excitations

In Fig. 4 we show two Brillouin spectra from the unpatterned (a) and patterned (b) areas with a field $H=1.5\,\mathrm{kOe}$ applied along the direction of the short ellipse axis. The similarity of the two spectra is an indication that the magnetic excitations are *not* fundamentally different in the two areas. The field dependence of the frequency of the two clearly observed modes is plotted, for the two orthogonal field directions, in Figs. 5(a) and 5(b) for the unpatterned and patterned areas, respectively. Consistent with the magnetization results, the frequencies in the unpatterned area are marginally higher when the field is along the easy axis (short ellipse axis) and noticeably higher in the patterned region when the

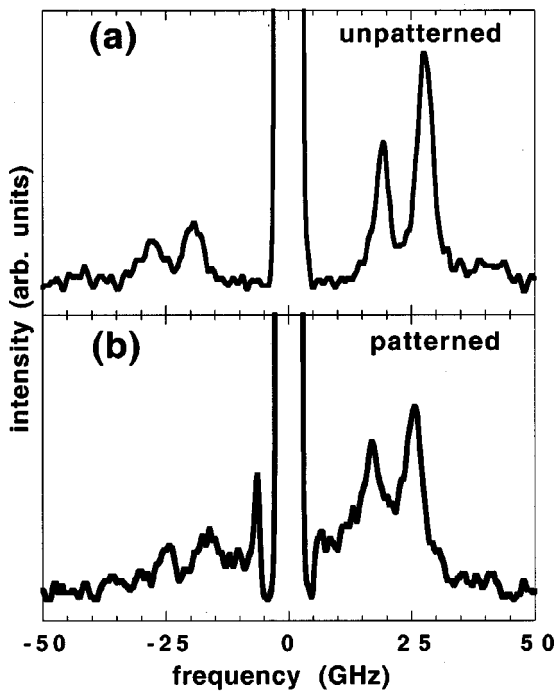

FIG. 4. Brillouin spectra from the (a) unpatterned and (b) patterned areas of the sample. The applied field is 1.5 kG along the short axis of the ellipses.

field is along the long ellipse axis. A quantitative analysis of the results shown in Figs. 5 requires a number of approximations. Exact numerical solutions, which include both anisotropy and finite wave vector contributions, can be obtained for the excitations of a thin magnetic plate. However, since we do not have a complete knowledge of the anisotropy, this approach is not particularly illuminating. The origin of the uncertainty lies in the out-of-plane dependence of the anisotropy in Eq. (1). We define ϕ as the angle subtended by the magnetization and the surface normal in the plane perpendicular to the long axis of the ellipses. If the second term in Eq. (1) is multiplied by $\cos^2(\phi)$, and $K<0$, the equation describes the energy of an easy plane magnet with the hard axis along the (in-plane) short ellipse axis. If it is not multiplied by $\cos^2(\phi)$ and $K<0$, Eq. (1) describes an easy axis magnet along the (in-plane) long axis of the ellipses. Which form is suitable to our film is not known. On the upside it turns out that, because $K \ll 4\pi M$, the frequencies obtained with the two forms do not differ greatly. For simplicity we shall use Eq. (1).

The two intense modes in spectrum Fig. 4(a) are the Damon-Eshbach[10] (surfacelike) magnon and the lowest order standing spin wave. Both modes are related to the FMR resonance frequency of an infinite plate. The FMR frequency resulting from Eq. (1) (and shape anisotropy) is

$$\omega=[(H+4\pi M)(H\pm 2K)]^{1/2}, \tag{2}$$

where the $\pm$ corresponds to the field applied along the easy and hard axes, respectively. In the absence of anisotropy the first order spin wave frequency is obtained by replacing H by $H+D(\pi/L)^2$, where D is the spin wave stiffness constant and L is the film thickness.[11] Provided that both the anisot-

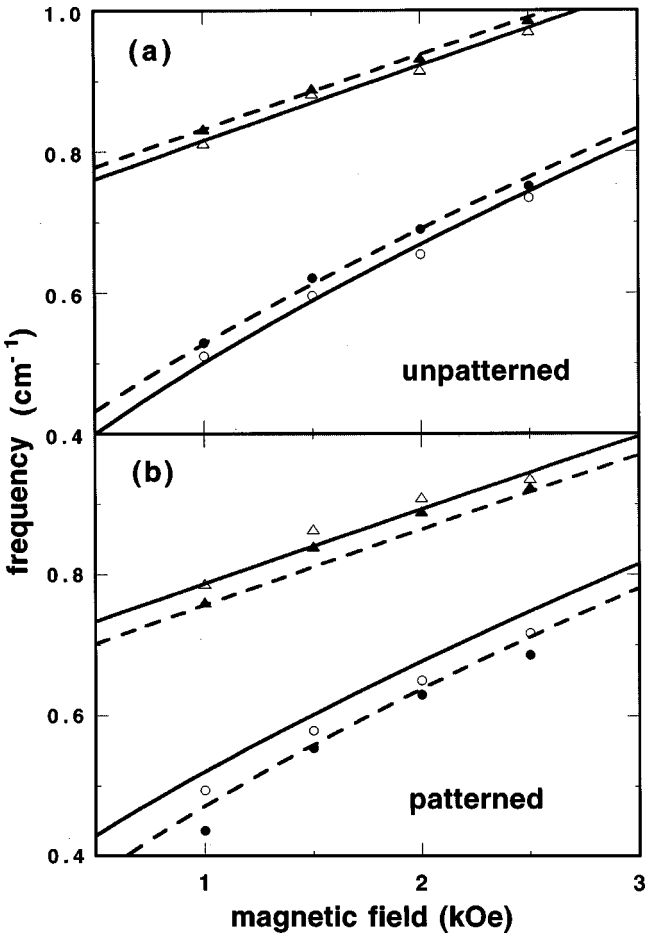

FIG. 5. Magnon frequencies in the (a) patterned and (b) unpatterned areas vs applied field. The triangles and dots indicate surface and bulk magnons, respectively. Open and full symbols correspond to the field along the long and short ellipse axes.

ropy and the finite wave vector contributions are small it appears reasonable to approximate the frequency by

$$\omega=[(H+D(\pi/L)^2+4\pi M)(H+D(\pi/L)^2\pm 2K)]^{1/2}. \tag{3}$$

The surface magnon frequency, again when K is zero, is given by

$$\omega^2=[(H+4\pi M)H]+(2\pi M)^2[1-\exp(-2qL)], \tag{4}$$

where q is the wave vector component parallel to the film surface. We again generalize Eq. (4) to include anisotropy by writing

$$\omega^2=[(H+4\pi M)(H\pm 2K)]+(2\pi M)^2[1-\exp(-2qL)]. \tag{5}$$

The data in Fig. 5(a), when fitted to Eqs. (3) and (5), yields $L=64$ nm, $4\pi M=16.8$ kG, and $K/M=40$ G. The full lines in the figure correspond to the fit. The value of L is consistent with our deposition conditions, $4\pi M$ and K are in the range typically obtained for sputtered Fe films, and K also agrees with the magnetization results in Fig. 2(a). Applying the same fitting procedure to the results from the patterned area, produce a lower quality fit as seen in Fig. 5(b). In this fit we have kept L fixed at 64 nm and obtain $4\pi M=15.3$ kG and $K/M=-60$ G. The value of $4\pi M$ is reasonable, and we do observe the reversal in the sign of K, however, its value is only in marginal agreement with the -250 G obtained from the magnetization.

We conclude from the above results that the approximation, to treat the hole array as an anisotropic homogeneous film, is reasonably successful but cannot be expected to produce an accurate quantitative description. Clearly a full treatment of the problem is required to produce quantitative agreement between theory and experiment.

Diffracted MOKE

We return now to the diffracted MOKE loops shown in Figs. 2 and 3. In Ref. 5 relatively subtle differences between the zeroth and first order diffracted loops were interpreted as due to the formation of domains. In the present case, our different-order hard axis loops (Fig. 3), show very pronounced differences. Equation (4) in Ref. 5 (note that the squaring of the whole expression as given there is incorrect) shows that the Kerr intensity is proportional to m_y, i.e., the component of magnetization perpendicular to the plane of incidence. The assumption in the derivation was that M, across each unit cell of the array, is uniform. For conventional MOKE (i.e., for the reflected beam) the expression remains valid simply by replacing M by the average value of m_y. For diffracted MOKE it can be shown that M must be replaced by a magnetic form factor given by

$$f=\int_S m_y \exp[iqr]dS, \tag{6}$$

where q is the wave vector transfer appropriate for each diffraction spot, r is the position within the cell, and the integration is carried out over a unit cell of the array. Note that for $q=0$ (i.e., the reflected spot) Eq. (6) is just the integral of m_y).

In Fig. 6(a) we show a schematic of the unit cell of our array. An expedient way in which to calculate the integral of Eq. (6) is to replace the unit cell by a matrix of ones and zeros as shown in Fig. 6(b) and to perform the simple summation corresponding to Eq. (6). This leads to $f_0=0.83$, $f_1=0.06$, and $f_2=0.031$; where the subindex denotes the diffraction order, and the values of f have been normalized to the form factor of a unit cell with no hole.

In order to calculate the form factor for the case when domains are present it is necessary to know the domain structure. Since the domain structure is not known, it is necessary to choose a domain structure and, a posteriori, see if it consistent with the experimental results. The structure we have chosen is based on the following two observations. Blade domains are known to form around voids in bulk materials.[12] (These domains are roughly triangular, have walls at $\sim 45°$ to the field, and magnetization perpendicular to the field). The D-MOKE results on a circular antidot array (Ref. 5) were found to be qualitatively consistent with the formation of such domains. In the present sample one might guess that the triangular domains between ellipses along a diagonal might coalesce to form a diagonal band. This conjecture is supported by LSTEM images that demonstrate the formation of diagonal magnetic domains in these samples as illustrated in Fig. 7.

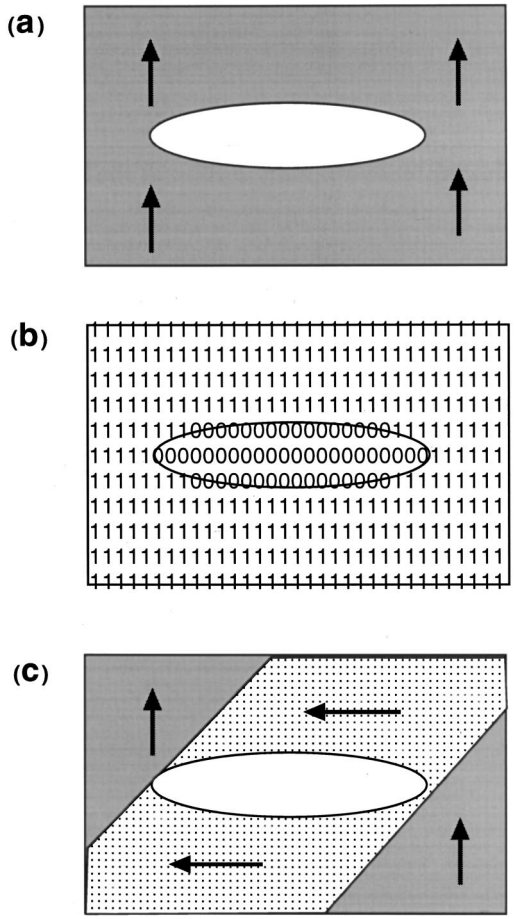

FIG. 6. Diagram of the (a) unit cell of the array, (b) matrix approximation used for calculating the form factor, and (c) inferred domain structure during switching.

A schematic of a unit cell with such a domain is shown in Fig. 6(c). Note that these domains almost eliminate the ''magnetic surface charges'' on the elliptical holes so that their formation is simply a result of the relative contributions of domain wall energy and surface induced magnetostatic fields. The relevant form factors, obtained by replacing the area of the domain with zeros in Fig. 6(b), leads to $f_0'=0.34$, $f_1'=0.14$, and $f_2'=0.027$.

The meaning of the above form factors is as follows: the ratio of f_1'/f_1 represents the ratio of Kerr intensities when domains are fully formed, to that at saturation. The zeroth order loop is therefore predicted to decrease to 40% of its saturation value at around zero applied field; experimentally it is slightly less than this. The first order loop is predicted to *increase* to more than twice its saturation value in excellent agreement with experiment. The second order loop is not expected to change much between saturation and zero field, again in very good agreement with the experimental results.

In order to use the form factor approach to describe the full loop it would be necessary to know the field dependence of domain formation. Since this is again not known, only a qualitative description can be provided. In Fig. 8 two hypothetical hysteresis loops are shown by dotted lines. They were chosen to be similar in shape to that in Fig. 3(d) (where form factor effects are small) and their amplitudes are in the ratio 1:2 roughly the ratio of the form factors with and without domains for the zeroth (0.34:0.83) and first (0.06:0.14) order diffraction loops given above. These dotted loops are the loops that would be obtained if the form factor were independent of field. The large dots on the figure represent the locations at which the domain structure, and hence the form factors, are known. In Fig. 8(a) we mimic the zeroth order loop: at high fields, where there are no domains, the real loop must coincide with the outermost loop, i.e., large form factor. At small fields, when domains are present, it must lie on the smaller loop (small form factor). For the first order loop, mimicked in Fig. 8(b), the ''high field'' dots are on the inner loop (small form factor). The dots at small fields, on the outer loops, assume that the domains are fully formed. How the system evolves from one loop to the other will depend on how the domains nucleate and vanish, but the evolution must remain between the two limiting (dotted)

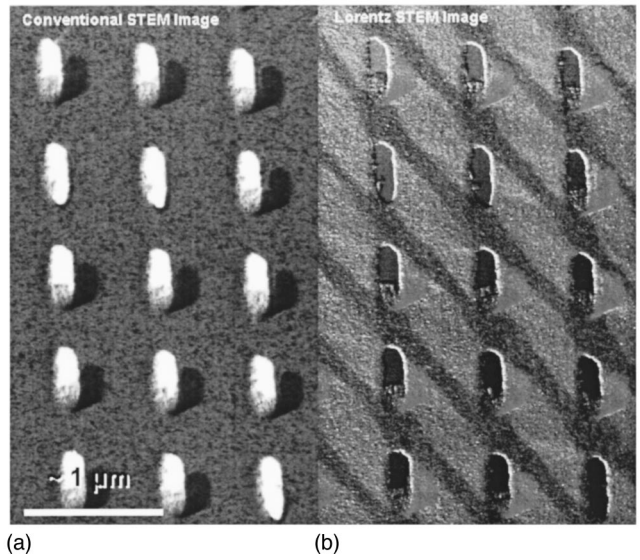

FIG. 7. (a) Conventional STEM image of the hole array. (b) Lorentz STEM image of the Fe hole array showing the existence of magnetic domains pinned by the holes in the film.

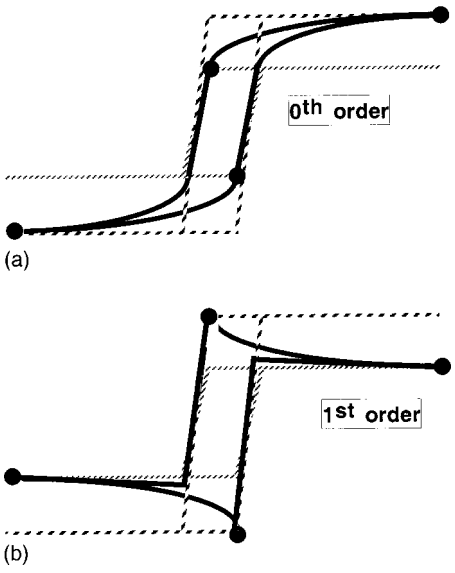

FIG. 8. D-MOKE loops corresponding to Figs. 3(b) and 3(c), calculated as described in the text.

loops. The full lines are guides to the eye as to how domain nucleation might evolve. The resulting loops bear a strong resemblance to those shown in Figs. 3(b) and 3(c) and thus provide confirmation that the inferred domain structure is a reasonable first approximation to describing the reversal in this negative array.

CONCLUSIONS

The magnetic properties, magnetization and magnetic excitations, of a hole array of ellipses were investigated using MOKE, LSTEM and Brillouin scattering. Both these properties are reasonably well explained by treating the system as an anisotropic uniform film. However, small deviations between experiment and the simple model indicate that a full theoretical treatment is required.

The magnetization reversal process, investigated by LSTEM and diffracted-MOKE, allows the domain structure during switching to be studied. An extension of the theory for D-MOKE, which describes the Kerr intensities in terms of a magnetic form factor, explains the overall shape of the D-MOKE loops and even allows a semiquantitative estimate of the size of the domains that exist during reversal.

ACKNOWLEDGMENTS

This work was supported by the U.S. Department of Energy, BES, Materials Science under Contract No. W-31-109-ENG-38. I.G. wishes to acknowledge DF/UFC and CNPq for support during his stay at ANL.

*Permanent address: Departamento de Fisica–UFC, Caixa Postal 6030, Campus do Pici, 60455-760-Fortaleza, CE, Brazil.

[1] C. A. Grimes, P. L. Trouilloud, J. K. Lumpp, and G. C. Bush, J. Appl. Phys. **81**, 4720 (1997).

[2] R. P. Cowburn, A. O. Adeyeye, and J. A. Bland, Appl. Phys. Lett. **70**, 2309 (1997); J. Magn. Magn. Mater. **173**, 193 (1997).

[3] Y. Otani, S. G. Kim, T. Kohda, K. Fukamichi, O. Kitakami, and Y. Shimada, IEEE Trans. Magn. **34**, 1090 (1998).

[4] L. Torres, L. Lopez-Diaz, and J. Iñiguez, Appl. Phys. Lett. **73**, 3766 (1998).

[5] P. Vavassori, V. Metlushko, R. M. Osgood, M. Grimsditch, U. Welp, and G. Crabtree, Phys. Rev. B **59**, 6337 (1999).

[6] L. Torres, L. Lopez-Diaz, O. Alejos, and J. Iñiguez, J. Appl. Phys. **85**, 6208 (1999).

[7] C. T. Yu, H. Jiang, L. Shen, P. J. Flanders, and G. J. Mankey, J. Appl. Phys. **87**, 6322 (2000).

[8] J. Sandercock, in *Light Scattering in Solids III*, edited by M. Cardona and G. Güntherodt, Topics in Appl. Phys. Vol. 51 (Springer, New York, 1982).

[9] N. J. Zaluzec (unpublished).

[10] K. W. Damon and J. R. Eshbach, J. Phys. Chem. Solids **19**, 308 (1961).

[11] A. Morrish, *The Physical Principles of Magnetism* (Wiley, New York, 1965).

[12] S. Chicazumi and S. Charap, *Physics of Magnetism* (Wiley, New York, 1964).